

Infrared Spectra of $\text{CH}_3\text{-NbF}$, $\text{CH}_2\text{=NbHF}$, and $\text{CH}\equiv\text{NbH}_2\text{F}^-$ Formed by Reaction of Methyl Fluoride with Laser-Ablated Niobium Atoms

Han-Gook Cho and Lester Andrews*

Department of Chemistry, University of Incheon, 177 Dohwa-dong, Nam-ku, Incheon, 402-749, South Korea, and Department of Chemistry, University of Virginia, P.O. Box 400319, Charlottesville, Virginia 22904-4319

Received September 7, 2005

Simple methyl, methyldiene, and anionic methyldiyne niobium complexes ($\text{CH}_3\text{-NbF}$, $\text{CH}_2\text{=NbHF}$, and $\text{CH}\equiv\text{NbH}_2\text{F}^-$) are produced in reactions of laser-ablated niobium atoms and methyl fluoride and isolated in an argon matrix. All three products are formed by co-deposition of the metal atoms and methyl fluoride, but the methyldiene complex is heavily favored. The methyldiene concentration increases further following visible and UV irradiations, whereas the methyl and methyldiyne complexes are depleted on visible and UV irradiations, respectively. This work reports the first experimental evidence for a group V anionic methyldiyne complex ($\text{CH}\equiv\text{NbH}_2\text{F}^-$), which is eliminated by the addition of CCl_4 to capture electrons formed in the ablation process. The DFT calculations show that one of the α -hydrogen atoms in $\text{CH}_2\text{=NbHF}$ is considerably bent toward the metal atom, an evidence of strong agostic interaction in the doublet ground state and provide isotopic frequencies for matching with observed values.

Introduction

Recent studies in our laboratories have shown that the early transition metals in groups IV and VI react with methyl halides and methane to produce simple methyldiene ($\text{CH}_2\text{=MHX}$, X = H, F, Cl, and Br) and methyldiyne ($\text{CH}\equiv\text{MH}_2\text{X}$) complexes along with the metal methyl hydride or halide ($\text{CH}_3\text{-MX}$) complexes.^{1–11} The products often form a photoreversible system via α -hydrogen migration^{1,4,8,10,11} or matrix configuration.^{2,5,6} These high-oxidation state complexes provide a simple model system to study substituent effects.

Electronic structure calculations using large basis sets show that the CH_2 group of the methyldiene complex is considerably distorted^{1–12} and that in the case of $\text{CH}_2\text{=MH}_2$ complexes the two metal–hydrogen bonds are not equivalent.^{5–9,11} The effect of agostic distortion is manifested in the infrared spectra of the methyldiene complexes formed from CH_2D_2 .^{5–9} Earlier theoretical studies using minimum basis sets failed to characterize the

agostic distortion,^{13–15} and more recent multiconfiguration calculations fixed the C_{2v} structure and found it to be stable.^{16,17}

High oxidation state transition metal complexes containing multiple metal–carbon bonds were first discovered in the form of Ta alkylidenes in 1970s.¹⁸ These complexes play important roles in alkane activation and catalytic metathesis of alkenes, alkynes, and cyclic compounds. They are also called Schrock carbenes or carbynes and are typically generated by intramolecular α -hydrogen elimination from a bis(alkyl) precursor.^{18,19} Bulky substituents are necessary to stabilize the electron-deficient metal center, and many of these d^0 -complexes are known to be agostic. Niobium methyldiene complexes have been mostly synthesized via α -hydrogen abstraction reactions,¹⁸ and one-electron oxidation of a dibenzyl niobium(IV) complex led to a cationic Nb(V) benzyldiene complex in tetrahydrofuran solution.²⁰ An anionic Nb methyldiene complex was prepared by the unusual bimetallic cleavage of a carbon–oxygen bond on a silica surface.²¹ Tantalum alkylidyne complexes have been prepared using trimethylphosphine ligands,²² but we have found no experimental evidence for a niobium alkylidyne complex or a group V methyldiyne anion complex.

In this investigation, reactions of laser-ablated niobium atoms with methyl fluoride diluted in argon were carried out, and the

* To whom correspondence should be addressed. E-mail: lsa@virginia.edu.

(1) Cho, H.-G.; Andrews, L. *J. Phys. Chem. A* **2004**, *108*, 6294 (Ti + CH_3F).

(2) Cho, H.-G.; Andrews, L. *J. Am. Chem. Soc.* **2004**, *126*, 10485 (Zr + CH_3F).

(3) Cho, H.-G.; Andrews, L. *Organometallics* **2004**, *23*, 4357 (Hf + CH_3F).

(4) Cho, H.-G.; Andrews, L. *Inorg. Chem.* **2005**, *44*, 979 (Ti + CH_3X).

(5) Andrews, L.; Cho, H.-G.; Wang, X. *Angew. Chem., Int. Ed.* **2005**, *44*, 113 (Zr + CH_4).

(6) Cho, H.-G.; Wang, X.; Andrews, L. *J. Am. Chem. Soc.* **2005**, *127*, 465 (Zr + CH_4).

(7) Cho, H.-G.; Wang, X.; Andrews, L. *Organometallics* **2005**, *24*, 2854 (Hf + CH_4).

(8) Cho, H.-G.; Andrews, L. *J. Am. Chem. Soc.* **2005**, *127*, 8226 (Mo + CH_4).

(9) Andrews, L.; Cho, H.-G.; Wang, X. *Inorg. Chem.* **2005**, *44*, 4834 (Ti + CH_4).

(10) Cho, H.-G.; Andrews, L. *Chem. Eur. J.* **2005**, *11*, 5017 (Mo + CH_3F).

(11) Cho, H.-G.; Andrews, L. *Organometallics* **2005**, *24*, 5678 (W + CH_3F).

(12) Ujaque, G.; Cooper, A. C.; Maseras, F.; Eisenstein, O.; Caulton, K. G. *J. Am. Chem. Soc.* **1998**, *120*, 361.

(13) Franci, M. M.; Pietro, W. J.; Hout, R. F., Jr.; Hehre, W. J. *Organometallics* **1983**, *2*, 281.

(14) Franci, M. M.; Pietro, W. J.; Hout, R. F., Jr.; Hehre, W. J. *Organometallics* **1983**, *2*, 815.

(15) Dobbs, K. D.; Hehre, W. J. *J. Am. Chem. Soc.* **1986**, *108*, 4663.

(16) Cundari, T. R.; Gordon, M. S. *J. Am. Chem. Soc.* **1992**, *114*, 539.

(17) Chung, G.; Gordon, M. S. *Organometallics* **2003**, *22*, 42.

(18) Schrock, R. R. *Chem. Rev.* **2002**, *102*, 145.

(19) Buchmeiser, M. R. *Chem. Rev.* **2000**, *100*, 1565.

(20) Duncalf, P. J.; Harrison, R. J.; McCamley, A.; Royan, B. W. *J. Chem. Soc., Chem. Commun.* **1995**, 2421.

(21) Caselli, A.; Solari, E.; Scopelli, R.; Floranti, C. *J. Am. Chem. Soc.* **1999**, *121*, 8296.

(22) McLain, S. J.; Wood, C. D.; Messerle, L. W.; Schrock, R. R.; Hollander, F. J.; Youngs, W. J.; Churchill, M. R. *J. Am. Chem. Soc.* **1978**, *100*, 5962.

products isolated in an argon matrix were investigated by means of infrared spectroscopy. Results indicate that at least three reaction products are formed on the basis of the behaviors of the absorptions upon photolysis, annealing, and the addition of CCl_4 to scavenge electrons. These are niobium methyl, methyldiene, and methyldyne complexes, and $\text{CH}\equiv\text{NbH}_2\text{F}^-$ is the first example of a niobium methyldyne anion complex.

Experimental and Computational Methods

Laser-ablated niobium atoms (Johnson-Matthey) were reacted with CH_3F (Matheson), CD_3F (synthesized from CD_3Br and HgF_2), and $^{13}\text{CH}_3\text{F}$ (Cambridge Isotopes, 99%) in excess argon during condensation at 8 K using a closed-cycle He refrigerator (Air Products). The methods are previously described in detail elsewhere.^{23–25} Concentrations of gas mixtures are typically 0.2–0.5% in argon. In addition, CCl_4 was added (0.05%) to the gas mixture in several experiments to capture electrons produced in the laser-ablation process.²⁴ After reaction, infrared spectra were recorded at a resolution of 0.5 cm^{-1} using a Nicolet 550 spectrometer with an MCT type B detector. Samples were later irradiated by a mercury arc lamp (175 W) with a combination of optical filters and were annealed, and more spectra were recorded.

Complementary density functional theory (DFT) calculations were carried out using the Gaussian 98 package,²⁶ B3LYP density functional, and 6-311++G(3df,3pd) basis sets for C, H, F, and SDD pseudopotential and basis set for Nb to provide a consistent set of vibrational frequencies for the reaction products. Structures were fully relaxed during optimization, and the optimized geometries were confirmed by vibrational analysis. All of the vibrational frequencies were calculated analytically. In calculation of the binding energy of a metal complex, the zero-point energy is included.

Results and Discussion

Three sets of product absorptions are found on the basis of the behaviors upon photolysis, annealing, and the addition of CCl_4 to trap ablated electrons, and they listed in Table 1 and compared with calculated potential reaction product values in Tables 2–4. Figure 1 shows the IR spectra in the regions of 1670–1730, 1510–1580, 670–790, and 530–660 cm^{-1} for laser-ablated Nb atoms co-deposited with $\text{Ar}/\text{CH}_3\text{F}$ and trace of CCl_4 at 8 K, trace (a), and the IR spectra in the same regions for Nb atoms with $\text{Ar}/\text{CH}_3\text{F}$ and their variation upon photolysis and annealing, traces (b–f). In addition, a very weak NbO_2 absorption ($A = 0.002$) at 876.0 cm^{-1} was detected.²³

$\text{CH}_3\text{-NbF}$. Two weak absorptions are observed overlapping at 627.4 and 629.7 cm^{-1} (marked I) in Figure 1. They are observed after deposition both with and without a trace of CCl_4 (Figure 1a,b) but disappear almost completely upon visible ($>530\text{ nm}$) irradiation and later reform slightly at the early stage of annealing. No other absorptions show the same spectroscopic

Table 1. Frequencies of Product Absorptions Observed from Reactions of Methyl Fluoride with Nb in Excess Argon^a

group	CH_3F	CD_3F	$^{13}\text{CH}_3\text{F}$	description
I	629.7, 627.4	629.2, 627.8	629.3, 627.2	Nb–F str
II	1698.7 , 1681.7	1220.9 , 1208.3	1698.6 , 1681.8	Nb–H str
	777.7, 772.9	695.8, 683.8	758.6	C=Nb str
	694.3	634.3, 632.3	693.9, 691.4	CNbH bend
	651.0 , 646.1	537.3 , 535.1	645.8 , 640.8	CH_2 wag
	612.4		611.3	Nb–F str
III	1560.4	1120.4	1560.3	NbH_2 str
	1526.7	1103.0	1526.7	NbH_2 str
	899.4		872.3	C=Nb str
	617.8	573.0	617.1	Nb–F str
	547.9		545.7	NbCH bend
	512.0		512.0	NbH_2 deform

^a All frequencies are in cm^{-1} . Stronger absorptions are bold. Description gives major coordinate.

characteristics upon photolysis, annealing, and the addition of CCl_4 . They exhibit small ^{13}C and D isotopic shifts as given in Table 1, indicating that the absorptions arise from a vibrational mode involving small carbon and hydrogen displacements.

Recent studies on reactions of transition metals with methyl halides find that $\text{CH}_3\text{-MX}$ is in many cases one of the major products,^{1,2,4,6,8,9} and calculations also show that the methyl transition-metal halide is one of the most plausible and stable products. In contrast, $\text{CH}_2\text{F-NbH}$ is 72 kcal/mol higher in energy than $\text{CH}_3\text{-NbF}$ both in quartet electronic states. Accordingly, geometry optimization starting from methyl fluoride and a transition-metal atom located nearby normally ends up with the structure $\text{CH}_3\text{-MX}$. The lone electron pairs on the halogen atom attract the electron-deficient transition metal atom and also provide a way to form a carbon–metal bond. Moreover, $\text{CH}_3\text{-MX}$ is normally very photoreactive,^{1,4,6,8} and the product easily rearranges by $\alpha\text{-H}$ transfer upon visible or UV irradiation.

The absorptions at 627.4 and 629.7 cm^{-1} are assigned to matrix site-split Nb–F stretching absorptions of $\text{CH}_3\text{-NbF}$ (Table 2). The Nb–F stretching absorption of $\text{CH}_3\text{-NbF}$ is predicted to be the strongest mode (the second strongest one is 20% as intense) with frequency 639.5 cm^{-1} ^{13}C and D isotopic shift of 0.1 and 0.5 cm^{-1} (Table 2). The fluorine stretching frequency of the NbF diatomic molecule (quintet state) is predicted to be 635.5 cm^{-1} at the current level of theory. Vibrational studies of niobium fluorides are sparse. The Nb–F stretching absorptions of solid NbF_4 are observed at 520, 605, and 650 cm^{-1} ,²⁷ and those of gaseous NbF_5 are at 683, 726, and 756 cm^{-1} .²⁸ In fact, the sharp, weak absorption at 589.8 cm^{-1} , which shows no precursor isotopic shift, is possibly due to the NbF diatomic molecule in solid argon. No gas-phase data are available.²⁹

As in previous studies of methyl fluoride reactions with transition metals,^{1–4} the absorptions of CH_3F fragments, produced by UV emission from the vaporized metal plume, are also observed in the infrared spectra. Jacox and Milligan investigated the infrared spectra of CH_2F , CHF, and CF radicals produced by vacuum UV photolysis of methyl fluoride and isolated in a solid argon matrix.³⁰ Infrared absorptions from CH_2F , CHF, and CF are observed in this work, consistent with

(27) Dickson, F. E. *J. Inorg. Nucl. Chem.* **1969**, *31*, 2636 (NbF_4).

(28) Boghosian, S.; Pavlatou, E. A.; Papatheodorou, G. N. *Vib. Spectrosc.* **2005**, *37*, 133 (NbF_5).

(29) The gas-phase infrared emission spectrum of VF (Ram, R. S.; Bernath, P. F.; Davis, S. P. *J. Chem. Phys.* **2002**, *116*, 7035) gives a ground-state frequency of 665 cm^{-1} . Considering that VO has a higher fundamental (Chertihin, G. V.; Bare, W. D.; Andrews, L. *J. Phys. Chem. A* **1997**, *101*, 5090) than NbO ,²³ the present 589.9 cm^{-1} band is reasonable for NbF red shifted slightly by the argon matrix.

(23) Zhou, M. F.; Andrews, L. *J. Phys. Chem. A* **1998**, *102*, 8251.

(24) Andrews, L.; Citra, A. *Chem. Rev.* **2002**, *102*, 885 and references therein.

(25) Wang, X.; Andrews, L. *J. Phys. Chem. A* **2003**, *107*, 570.

(26) Frisch, M. J.; Trucks, G. W.; Schlegel, H. B.; Scuseria, G. E.; Robb, M. A.; Cheeseman, J. R.; Zakrzewski, V. G.; Montgomery, J. A., Jr.; Stratmann, R. E.; Burant, J. C.; Dapprich, S.; Millam, J. M.; Daniels, A. D.; Kudin, K. N.; Strain, M. C.; Farkas, O.; Tomasi, J.; Barone, V.; Cossi, M.; Cammi, R.; Mennucci, B.; Pomelli, C.; Adamo, C.; Clifford, S.; Ochterski, J.; Petersson, G. A.; Ayala, P. Y.; Cui, Q.; Morokuma, K.; Rega, N.; Salvador, P.; Dannenberg, J. J.; Malick, D. K.; Rabuck, A. D.; Raghavachari, K.; Foresman, J. B.; Cioslowski, J.; Ortiz, J. V.; Baboul, A. G.; Stefanov, B. B.; Liu, G.; Liashenko, A.; Piskorz, P.; Komaromi, I.; Gomperts, R.; Martin, R. L.; Fox, D. J.; Keith, T.; Al-Laham, M. A.; Peng, C. Y.; Nanayakkara, A.; Challacombe, M.; Gill, P. M. W.; Johnson, B.; Chen, W.; Wong, M. W.; Andres, J. L.; Gonzalez, C.; Head-Gordon, M.; Replogle, E. S.; Pople, J. A. *Gaussian 98*, Revision A.11.4; Gaussian, Inc.: Pittsburgh, PA, 2002.

Table 2. Observed and Calculated Fundamental Frequencies of $\text{CH}_3\text{-NbF}$ Isotopomers in the Ground $^4\text{A}'$ Electronic State^a

approx description	$\text{CH}_3\text{-NbF}$			$\text{CD}_3\text{-NbF}$			$^{13}\text{CH}_3\text{-NbF}$			
	obsd	calcd ^b	calcd ^a	int	obsd	calcd ^a	int	obsd	calcd ^a	int
ν_1 A' CH_3 str		3110.2	3114.7	1		2298.6	0		3104.7	1
ν_2 A' CH_3 str		2938.9	2943.8	3		2114.9	1		2940.0	4
ν_3 A' CH_3 scis		1407.9	1405.6	4		1020.5	3		1402.4	4
ν_4 A' CH_3 deform		1163.6	1160.3	14		914.5	24		1150.5	13
ν_5 A' Nb–F str	629.7	631.0	639.5	149	629.2	639.0	147	629.3	639.4	150
ν_6 A' C–Nb str		565.0	562.7	30		484.5	28		552.1	27
ν_7 A' CH_3 rock		380.3	381.6	28		311.0	14		375.8	28
ν_8 A' CNbF bend		143.8	145.3	2		135.3	2		144.7	2
ν_9 A' CH_3 str		2989.8	2996.3	4		2211.5	2		2986.2	4
ν_{10} A'' CH_3 scis		1415.6	1415.5	4		1027.4	3		1412.3	4
ν_{11} A'' CH_2 twist		366.2	365.7	5		272.4	3		364.0	5
ν_{12} A'' HCNbF distort		91.5	88.8	0		64.9	1		88.7	0

^a B3LYP/6-311++G(3df, 3pd)/SDD level. Frequencies and intensities are in cm^{-1} and km/mol . Infrared intensities are calculated values. ^b Frequencies computed using 6-311++G(2d, p) basis set.

Table 3. Observed and Calculated Fundamental Frequencies of $\text{CH}_2=\text{NbHF}$ Isotopomers in the Ground $^2\text{A}'$ Electronic State^a

approx description	$\text{CH}_2=\text{NbHF}$			$\text{CD}_2=\text{NbDF}$			$^{13}\text{CH}_2=\text{NbHF}$			
	obsd	calcd ^b	calcd ^a	int	obsd	calcd ^a	int	obsd	calcd ^a	int
ν_1 A' C–H str		3206.9	3209.9	3		2376.7	5		3198.9	3
ν_2 A' C–H str		2871.1	2809.3	4		2066.6	3		2832.5	4
ν_3 A' Nb–H str	1698.7 ^c	1722.6	1757.9	284	1220.9	1250.9	148	1698.6	1757.9	284
ν_4 A' CH_2 bend		1328.8	1334.7	21		1047.9	23		1325.5	20
ν_5 A' C=Nb str	777.7	800.1	810.6	72	683.8	711.1	47	758.6	792.0	79
ν_6 A' Nb–F str	694.3	729.7	727.3	87	632.3	666.3	133	691.4	723.1	81
ν_7 A' CNbH bend	612.4	634.5	632.9	56		516.6	3	611.3	632.1	54
ν_8 A' CH_2 rock		375.0	394.3	4		313.1	3		390.7	4
ν_9 A' CNbF bend		182.0	182.0	2		159.3	1		180.6	2
ν_{10} A'' CH_2 wag	651.0	702.1	710.7	93	537.3	557.6	63	645.8	704.6	91
ν_{11} A'' CH o-o-p bend		475.5	470.6	4		224.6	1		470.5	4
ν_{12} A'' NbH o-o-p bend		60.0	21.0	50		23.9	30		20.5	50

^a B3LYP/6-311++G(3df, 3pd)/SDD level. Frequencies and intensities are in cm^{-1} and km/mol . Infrared intensities are calculated values. ^b Frequencies computed using 6-311++G(2d, p) basis set. ^c Observed intensities (milliabsorbance units) for these bands (Figure 1d) are 18, 4.5, 12, 6.6, and 17, respectively, going down the column.

Table 4. Observed and Calculated Fundamental Frequencies of $\text{CH}\equiv\text{NbH}_2\text{F}^-$ Isotopomers in the Ground $^1\text{A}'$ Electronic State^a

approx description	$\text{CH}\equiv\text{NbH}_2\text{F}^-$			$\text{CD}\equiv\text{NbD}_2\text{F}^-$			$^{13}\text{CH}\equiv\text{NbH}_2\text{F}^-$			
	obsd	calcd ^b	calcd ^a	int	obsd	calcd ^a	int	obsd	calcd ^a	int
ν_1 A' C–H str		3115.0	3118.2	16		2311.4	0		3107.3	17
ν_2 A' NbH ₂ str	1560.4 ^c	1608.2	1618.7	432	1120.4	1150.5	211	1560.3	1618.6	433
ν_3 A' C≡Nb str	899.4	952.7	949.1	141		908.7	128	872.3	920.1	134
ν_4 A' NbH ₂ bend		631.0	625.7	45		473.4	14		624.0	113
ν_5 A' Nb–F str	617.8	628.7	622.5	291	573.0	576.5	174	617.1	621.6	222
ν_6 A' NbCH bend	547.9	548.0	563.3	96		424.9	114	545.7	560.6	92
ν_7 A' NbH ₂ wag		491.8	495.7	29		379.7	11		495.2	31
ν_8 A' CNbF bend		224.0	224.5	4		209.3	3		221.2	3
ν_9 A'' NbH ₂ str	1526.7	1569.2	1583.8	664	1103.0	1132.3	342	1526.7	1583.7	663
ν_{10} A'' CH o-o-p bend		656.8	647.1	17		522.5	15		650.8	16
ν_{11} A'' NbH ₂ deform	512.0	519.2	524.2	104		373.1	55	512.0	524.2	104
ν_{12} A'' NbH ₂ rock		331.1	322.5	14		246.4	5		322.3	14

^a B3LYP/6-311++G(3df,3pd)/SDD level. Frequencies and intensities are in cm^{-1} and km/mol . Infrared intensities are calculated values. ^b Frequencies computed using 6-311++G(2d,p)/SDD basis set. ^c Observed intensities (milliabsorbance units) for these bands (Figure 1c) are 3.2, 2.4, 3.4, 1.3, 5.1, and 0.8, respectively, going down the column.

previous studies.^{1–4,30} These absorptions remain almost unchanged in the process of photolysis and early stages of annealing.

$\text{CH}_2=\text{NbHF}$. In the region of 1670–1730 cm^{-1} , a strong diagnostic product absorption is observed at 1698.7 cm^{-1} (marked II) in the spectra both with and without trace of CCl_4 . The absorption increases about 70% upon visible (>420 nm) and another 100% following UV (240–380 nm) irradiations and sharpens on annealing up to 26 K and later decreases at higher temperature. The ^{13}C substitution leads to a negligible shift in frequency, whereas deuteration results in a large frequency shift to 1220.9 cm^{-1} (H/D isotopic ratio 1.391) as

shown in Figures 2 and 3, indicating that the band originates from a Nb–H stretching mode. In earlier studies, the stretching absorptions of binary niobium hydrides are observed in the same frequency region.^{31,32} Particularly the absorptions of the tetravalent NbH_4 were observed at 1683.9, 1688.4, 1705.2, and 1708.0 cm^{-1} , which are close but not the same as observed here.

The Nb–H stretching absorption indicates that C–H activation readily takes place by Nb in the reaction with CH_3F , but the direct C–H insertion product $\text{CH}_2\text{F-NbH}$ is much higher in energy than the $\text{CH}_3\text{-NbF}$ product likely first formed here. Electronic structure calculations show, however, that the most

(30) Jacox, M. E.; Milligan, D. E. *J. Chem. Phys.* **1969**, *50*, 3252.

(31) Van Zee, R. J.; Weltner, W., Jr. *J. Chem. Phys.* **1995**, *102*, 4367.
(32) Wang, X.; Andrews, L. Unpublished data (Nb + H₂).

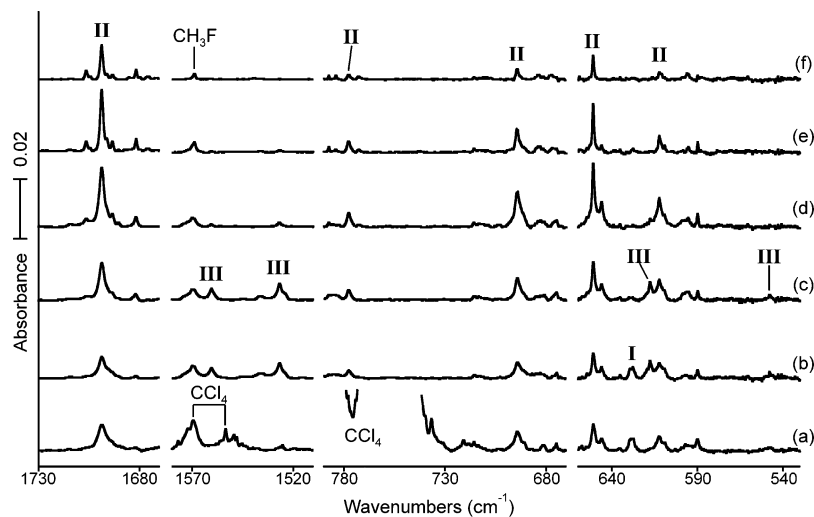


Figure 1. Infrared spectra in the regions of 1670–1730, 1510–1580, 670–790, and 530–660 cm^{-1} for laser-ablated Nb atoms co-deposited with CH_3F in excess argon at 8 K: (a) Nb + [0.5% CH_3F + 0.05% CCl_4] in Ar deposited for 1 h, (b) Nb + 0.5% CH_3F in Ar deposited for 1 h, (c) after broad-band irradiation with a filter ($\lambda > 530$ nm) for 30 min, (d) after broad-band irradiation with a filter ($240 < \lambda < 380$ nm) for 30 min, (e) after annealing to 26 K, and (f) after annealing to 32 K. I, II, or III indicates the product absorption group.

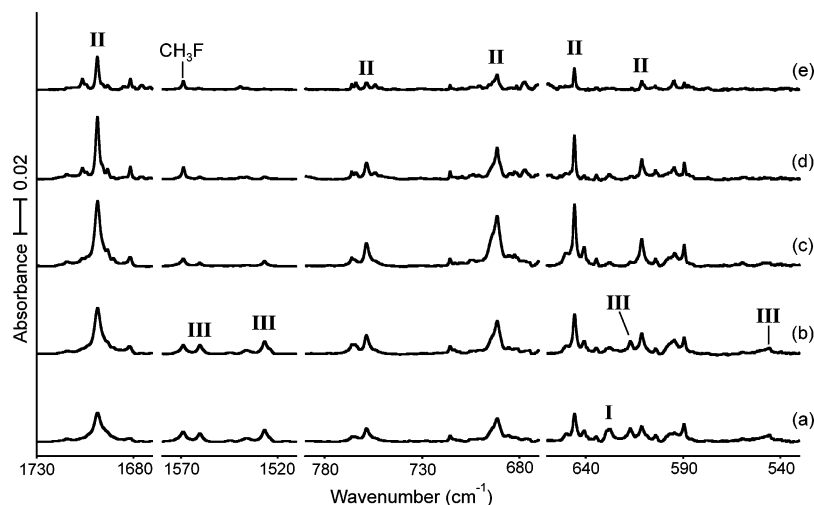


Figure 2. Infrared spectra in the regions of 1670–1730, 1510–1580, 670–790, and 530–660 cm^{-1} for laser-ablated Nb atoms co-deposited with $^{13}\text{CH}_3\text{F}$ in excess argon at 8 K: (a) Nb + 0.5% CH_3F in Ar deposited for 1 h, (b) after broad-band irradiation with a filter ($\lambda > 530$ nm) for 30 min, (c) after broad-band irradiation with a filter ($240 < \lambda < 380$ nm) for 30 min, (d) after annealing to 26 K, (e) after annealing to 32 K. I, II, or III indicates the product absorption group.

energetically favorable mono-hydrido product should be $\text{CH}_2=\text{NbHF}$ in the doublet ground state (Figure 4). The present result suggests that like group IV and VI transition metals, group V transition metals also form simple methylenes by reaction with CH_3F followed by α -H transfer. The formation of simple transition-metal methylenes ($\text{CH}_2=\text{MHX}$) in reactions of vaporized early transition-metal atoms and methyl halides or methane is straightforward.^{1–11}

The frequencies of $\text{CH}_2=\text{NbHF}$ isotopomers are predicted at the level of B3LYP/6-311++G(3df,3pd) and listed along with the observed values in Table 3. The calculated frequencies using the 6-311++G(2d,p) basis set are also listed for $\text{CH}_2=\text{NbHF}$ for comparison. (In most cases, the medium basis set gives better agreement than the large basis set.) The importance of polarization functions in calculation of methylenes has been demonstrated in a recent study; without polarization functions, the agostic structure is not reproduced.⁶ The agreement between the observed anharmonic and calculated harmonic values are appropriate for the very strong Nb–H stretching absorption (observed/calculated = 1698.7/1757.8 = 0.966),³³ and the predicted isotope shifts of 0.0 and -506.9 cm^{-1} on ^{13}C and D

substitutions are in accord with the observed values of 0.1 and -477.8 cm^{-1} again considering the effect of anharmonicity. Similar agreement was found for the M–H stretching modes of $\text{CH}_2=\text{ZrHF}$ and $\text{CH}_2=\text{MoHF}$.^{2,10} Unfortunately, the C–H stretching frequencies are too weak to be observed here (calculated 1% of the intensity of the Nb–H stretching frequency, Table 3).

Four product absorptions showing the same behavior upon photolysis, annealing, and addition of CCl_4 (group II) are also observed (marked II) in lower frequency regions of Figures 1–3. The absorption at 777.7 cm^{-1} in Figure 1 shows isotope shifts of -19.1 and -93.9 cm^{-1} by ^{13}C and D substitutions ($^{12}\text{C}/^{13}\text{C}$ and H/D isotopic ratios of 1.025 and 1.137). The relatively large ^{13}C isotopic shift indicates that the band arises from a mostly carbon-metal stretching mode, but the D shift shows that H motion is also involved. In this low symmetry molecule, normal modes involve extensive internal coordinate mixing. The calculated frequency of 810.6 cm^{-1} and the ^{13}C and D isotope shifts of -18.0 and -99.5 cm^{-1} for this mixed C=Nb stretching

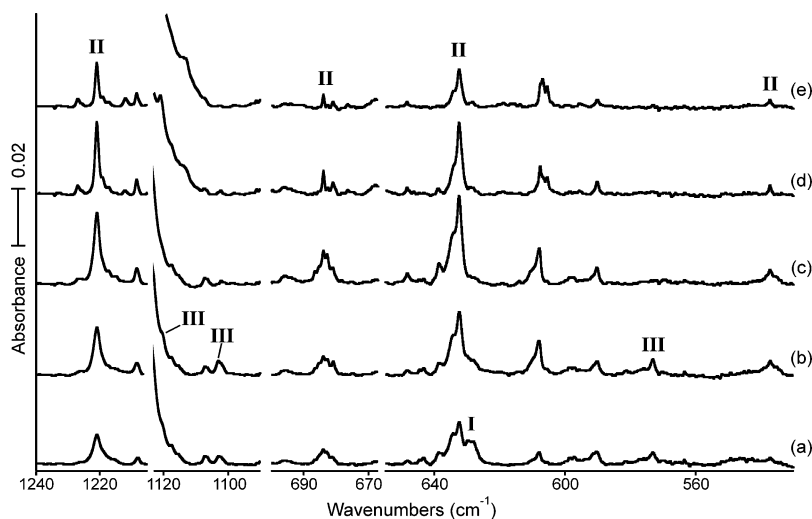


Figure 3. Infrared spectra in the regions of 1205–1240, 1090–1123, 667–700, and 530–655 cm^{-1} for laser-ablated Nb atoms co-deposited with CD_3F in excess argon at 8 K. (a) Nb + 0.5% CD_3F in Ar deposited for 1 h, (b) after broad-band irradiation with a filter ($\lambda > 530 \text{ nm}$) for 30 min, (c) after broad-band irradiation with a filter ($240 < \lambda < 380 \text{ nm}$) for 30 min, (d) after annealing to 26 K, and (e) after annealing to 32 K. I, II, or III indicates the product absorption group.

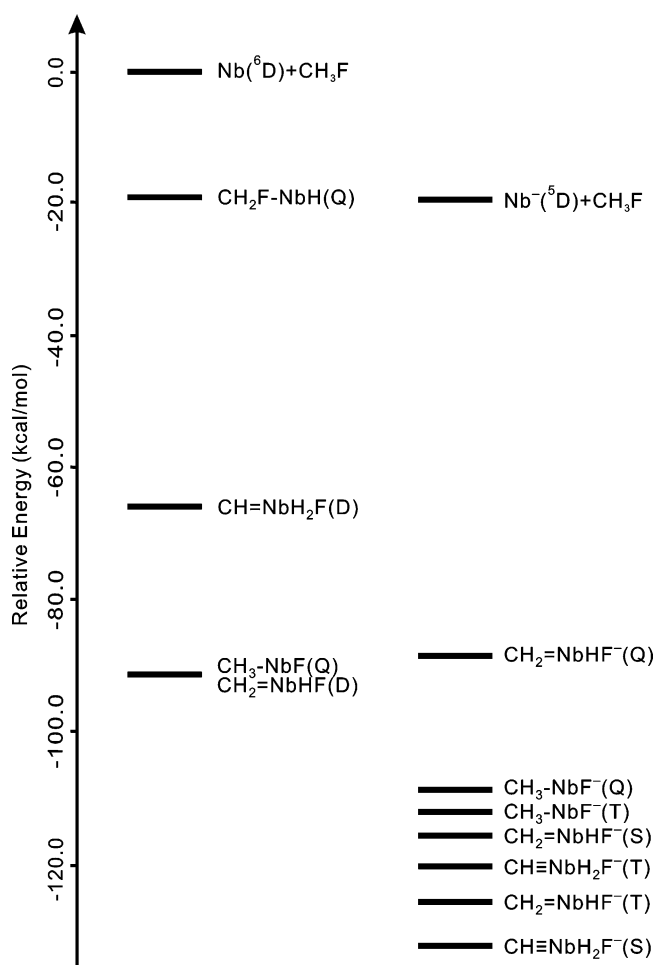


Figure 4. Computed (B3LYP/6-311++G(3df,3pd)/SDD) energies of neutral and anionic reaction products relative to $\text{Nb}(^6\text{D}) + \text{CH}_3\text{F}$. Note that $\text{CH}\equiv\text{NbH}_2\text{F}^-$ is the most stable among the plausible anion products. For the neutral products, D denotes doublet and Q quartet states, and for the anion products S denotes singlet, T triplet, and Q quintet states.

mode are in excellent agreement with the observed values. The much stronger absorption at 694.3 cm^{-1} in Figure 1 shows isotope shifts of -2.9 and -62.0 cm^{-1} by ^{13}C and D substitu-

tions ($^{12}\text{C}/^{13}\text{C}$ and H/D isotopic ratios of 1.004 and 1.098). On the basis of the frequency and relatively small isotope shifts on ^{13}C and D substitutions, the band is attributed to a vibrational mode with mostly Nb–F stretching character. The predicted frequency of 727.3 cm^{-1} and the ^{13}C and D isotope shifts of -4.2 and -61.0 cm^{-1} for the vibrational mode are again in excellent agreement with the observed values.

In the lower frequency region, another strong absorption with the same spectral behavior is observed at 651.0 cm^{-1} , which shows ^{13}C and D isotope shifts of -5.2 and -113.7 cm^{-1} ($^{12}\text{C}/^{13}\text{C}$ and H/D isotopic ratios of 1.008 and 1.212). The frequency, high intensity, and large deuterium shift suggest a CH_2 wagging mode: the frequency is predicted at 710.7 cm^{-1} and the ^{13}C and D isotope shifts -6.1 and -153.1 cm^{-1} , and the larger discrepancy between calculated and observed D shift is due to greater anharmonicity in the CH_2 wagging mode. Another absorption and its ^{13}C counterpart are observed at 612.4 and 611.3 cm^{-1} , without observation of the D counterpart. The band is attributed to the mostly CNbH bending mode. The calculated frequencies are 632.9 and 632.1 cm^{-1} , and that of the deuterated isotopomer is predicted at 557.6 cm^{-1} with a much lower intensity (about a twentieth) than those of the other isotopomers.

The five absorptions assigned here to $\text{CH}_2\text{=NbHF}$ (Table 3) correlate with calculated frequencies through scale factors (calculated/observed), and are 0.966, 0.959, 0.955, 0.968, and 0.916, respectively, using the large basis set. These are appropriate scale factors for this level of theory (the wagging mode is more anharmonic).³³ Note also that the observed and calculated infrared intensities (Figure 1d, Table 3) are qualitatively in agreement for these five modes although the Nb–F stretching mode is about twice as strong as predicted. (The more anharmonic wagging mode is stronger than predicted by our harmonic calculation.)

The observed spectroscopic evidence and computational results indicate that like group IV and VI transition metals, group V transition metals also activate the C–H bond of methyl halide and form a simple methyldene complex. The M–H stretching frequencies for these $\text{CH}_2\text{=MHF}$ molecules^{2,10} increase from 1537.8 to 1698.7 to 1797.7 cm^{-1} moving across the periodic table, just as the frequencies for the binary metal hydrides do.^{31,32,34,35}

$\text{CH}\equiv\text{NbH}_2\text{F}^-$. In the 1510–1580 cm^{-1} region, Figure 1b,c shows two product absorptions with about 2:1 intensity ratio at 1526.7 and 1560.4 cm^{-1} (marked III), but they are almost absent with a trace of CCl_4 present (Figure 1a). The observed absorptions slightly increase upon visible (>420 nm) photolysis, but deplete almost completely in the following UV (240–380 nm) irradiation. The ^{13}C substitution leads to negligible frequency shifts, while deuteration results in large frequency shifts of -423.7 and -440.0 cm^{-1} (H/D isotopic ratios of 1.384 and 1.393).

The isotope shifts suggest that the absorptions at 1526.7 and 1560.4 cm^{-1} arise from Nb–H stretching modes (probably a symmetric and antisymmetric pair) of another reaction product. This indicates again that Nb–H bond formation readily occurs; however, the frequencies are far lower than normal Nb–H stretching frequencies of neutral niobium hydrides.^{31,32} Earlier studies show that the concentration of an anionic product decreases dramatically on addition of CCl_4 , by removing electrons produced in the laser-ablation process.²⁴ Elimination of the absorptions by addition of CCl_4 , along with the exceptionally low hydrogen stretching frequencies, indicates that the absorptions at 1526.7 and 1560.4 cm^{-1} in fact originate from an anionic species with at least two hydrogen atoms bonded to the Nb center.

With addition of an electron to the Nb atom, it becomes isoelectronic to the Mo atom, having six electrons in the valence shell ($5s^14d^5$). In recent studies, we found that Mo forms methylidyne complexes as well as methylidene complexes in reactions with CH_3F and CH_4 .^{8,10} Moreover, the methylidyne and methylidene complexes are interconvertible via α -hydrogen migration on visible and UV photolyses. The most energetically favorable anionic product formed in the reaction of Nb and CH_3F with two Nb–H stretching absorptions is $\text{CH}\equiv\text{NbH}_2\text{F}^-$ in the singlet ground state as shown in Figure 4. The present results also suggest that photodetachment of an electron by UV irradiation gives the $\text{CH}=\text{NbH}_2\text{F}$ intermediate, which rearranges to the more stable $\text{CH}_2=\text{NbHF}$ methylidene complex and increases the intensities of its absorptions as shown in Figures 1–3.

Calculations show that $\text{CH}\equiv\text{NbH}_2\text{F}^-$ in the singlet ground state is quite stable (the binding energy relative to CH_3F and Nb^- (^5D) is 112 kcal/mol), but $\text{CH}=\text{NbH}_2\text{F}$ in the doublet ground state is 65 and 25 kcal/mol higher in energy than $\text{CH}\equiv\text{NbH}_2\text{F}^-$ and $\text{CH}_2=\text{NbHF}$, respectively as shown in Figure 4. Our computations also determine that $\text{CH}\equiv\text{NbH}_2\text{F}^-$ is the most stable among the plausible anionic products from Nb^- and CH_3F . The Nb–H stretching frequencies of $\text{CH}\equiv\text{NbH}_2\text{F}^-$ are predicted at 1583.8 and 1618.7 cm^{-1} , which are only slightly higher than the bands observed here for a new anionic species. The observed/calculated = 1526.7/1583.8 and 1560.4/1618.7 ratios are both 0.964 and are very near the 0.966 value for $\text{CH}_2=\text{NbHF}$. The computed shifts of 0.1 and 0.1 cm^{-1} for $^{13}\text{CH}\equiv\text{NbH}_2\text{F}^-$ are compared to the observed shifts of 0.0 and 0.1 cm^{-1} , and the calculated shifts of -451.5 and -468.2 cm^{-1} for $\text{CD}\equiv\text{NbD}_2\text{F}^-$ are compared to observed -423.7 and -440 cm^{-1} values, all in excellent agreement again considering the lack of anharmonic correction in the calculations. Finally, the C–H stretching mode is too weak ($<3\%$ of the stronger Nb–H stretching mode, Table 4) to be observed here.

Four absorptions for $\text{CH}\equiv\text{NbH}_2\text{F}^-$ are also observed in the lower frequency region (marked III) with the same behavior

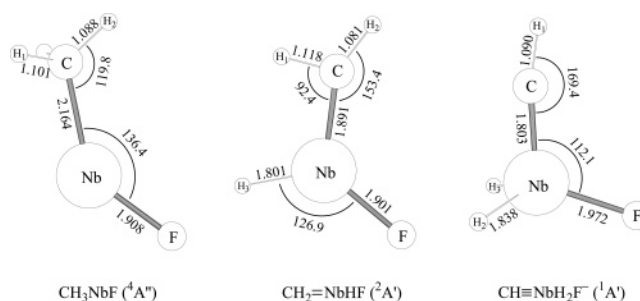


Figure 5. Optimized molecular structures (B3LYP/6-311++G-(3df,3pd)/SDD) of Nb-methyl fluoride complexes identified in this study. The bond lengths and angles are in Å and deg.

upon photolysis and addition of CCl_4 . The $\text{C}\equiv\text{Nb}$ stretching absorption is observed at 899.4 cm^{-1} (not shown) with a ^{13}C isotope shift of -27.1 cm^{-1} (the D counterpart is not observed), which is compared with the predicted 949.1 cm^{-1} frequency and ^{13}C shift of -29.0 cm^{-1} . The absorption at 617.8 cm^{-1} shows relatively small ^{13}C and D shifts of -0.7 cm^{-1} and -44.8 cm^{-1} ($^{13}\text{C}/^{12}\text{C}$ and H/D isotopic ratios of 1.001 and 1.078) and is attributed to the mostly Nb–F stretching mode, whose frequency is predicted 622.5 cm^{-1} with ^{13}C and D shifts of -0.9 and -46.0 cm^{-1} , again in excellent agreement with the observed values. Another absorption at 547.9 cm^{-1} shows a small ^{13}C shift of -2.2 cm^{-1} , without observation of the D counterpart. On the basis of the frequency and small ^{13}C shift, the band is assigned to the mostly NbCH bending mode, whose frequency is predicted 563.3 cm^{-1} with ^{13}C and D isotope shifts of -2.7 and -138.4 cm^{-1} . The D counterpart is apparently beyond our observation limit. On the further lower frequency side, a weak absorption is observed at 512.0 cm^{-1} with a negligible ^{13}C shift (not shown). The frequency and absent ^{13}C shift lead to the NbH_2 deformation, whose frequency is predicted at 524.2 cm^{-1} with no ^{13}C shift and D shift of -151.1 cm^{-1} .

The six absorptions assigned here to $\text{CH}\equiv\text{NbH}_2\text{F}^-$ (Table 4) are related to calculated frequencies by scale factors (calculated/observed), which are 0.964, 0.937, 0.992, 0.973, 0.964, 0.977, respectively, using the large basis set. These scale factors are near the scale factors for $\text{CH}_2=\text{NbHF}$, which shows that our B3LYP calculation works equally well for $\text{CH}\equiv\text{NbH}_2\text{F}^-$ and $\text{CH}_2=\text{NbHF}$. Also notice that calculated and observed infrared intensities (Figure 1c, Table 4) are in reasonable agreement and again the Nb–F stretching mode is relatively stronger than calculated.

The observed spectroscopic evidence and calculation results indicate that the anionic niobium methylidyne (carbyne) complex is indeed provided in the reaction of laser-ablated niobium atoms and CH_3F . Anionic carbyne complexes are rare. They are synthesized either from Schrock carbyne (methylidyne) complexes by substituting the α -hydrogen with a metal atom or from Fischer carbyne complexes by replacing one of the neutral ligands (e.g., CO) with an anion.¹⁸ Anionic carbynes are of interest due to their physical properties and reactivity as well as their bonding and electronic structures. The reported carbyne complexes are mostly group VI transition-metal complexes, and attempts to synthesize anionic group V carbyne complexes have not been successful. The $\text{CH}\equiv\text{NbH}_2\text{F}^-$ anion identified in this study is, therefore, not only the first niobium carbyne complex but the first anionic group V transition-metal carbyne complex to the best of our knowledge.¹⁸

Structures. The calculated molecular structures for the identified reaction products of CH_3F with Nb are illustrated in Figure 5. Note that the C–Nb bond length decreases with the increasing bond order (2.164, 1.891, and 1.803 Å for

(34) Chertihin, G. V.; Andrews, L. *J. Phys. Chem.* **1995**, *99*, 15004 (ZrH₄).

(35) Andrews, L. *Chem. Soc. Rev.* **2004**, *33*, 123 and references therein.

Table 5. Geometrical Parameters and Physical Constants of CH₃-NbF, CH₂=NbHF, and CH≡NbH₂F^{-a}

parameters	CH ₃ -NbF	CH ₂ =NbHF	CH≡NbH ₂ F ⁻
r(C-H ₁)	1.101	1.118	1.090
r(C-H ₂)	1.088	1.081	
r(C-Nb)	2.164	1.891	1.803
r(Nb-H ₃)		1.801	1.838
r(Nb-F)	1.908	1.901	1.972
r(Nb...H)	2.687	2.236	2.882
∠H ₁ CH ₂	108.5	114.3	
∠H ₂ CH ₃	107.0		
∠CNbF	136.4	121.7	112.1
∠CNbH ₃		111.4	101.3
∠H ₃ NbF		126.9	113.6
∠H ₁ CNb	106.2	92.4	169.4
∠H ₂ CNb	119.8	153.4	
Φ(H ₁ CNbH ₂)	113.6	180.0	121.5
Φ(H ₁ CNbF)	123.2	180.0	0.0
mol. symm	C _s	C _s	C _s
q(C) ^b	-0.91	-0.78	-1.09
q(H ₁) ^b	0.06	0.02	0.00
q(H ₂) ^b	0.03	0.00	-0.55
q(H ₃) ^b	0.06	-0.43	-0.55
q(Nb) ^b	1.33	1.80	1.88
q(F) ^b	-0.57	-0.61	-0.69
μ ^c	1.96	1.05	2.16
state ^d	4A''	2A'	1A'
ΔE ^e	91.9	92.0	131.8 (112.0) ^f

^a Bond lengths and angles are in Å and degrees. Calculated at the level of B3LYP/6-311++G(3df,3pd)/SDD. ^b Mulliken atomic charge. ^c Molecular dipole moment in D. ^d Electronic state. ^e Binding energies in kcal/mol relative to CH₃F and Nb (⁶D). ^f Binding energy in kcal/mol relative to CH₃F and ⁵Nb (⁵D).

CH₃-NbF, CH₂=NbHF, and CH≡NbH₂F⁻, respectively). The predicted C-Nb and C=Nb bond lengths are slightly shorter than 2.228 and 1.95–1.99 Å measured for Tp^{Me2}NbCl-(i-Pr)(PhC≡CMe) [Tp^{Me2} = hydrotris(3,5-dimethylpyrazolyl)-borate]³⁶ and typical Nb methyldene complexes,¹⁸ respectively. Both CH₃-NbF and CH≡NbH₂F⁻ have C_s symmetry, and CH₂=NbHF is predicted to be planar. While the calculated structure of CH≡NbH₂F⁻ is basically similar to the structure computed for CH≡MoH₂F¹⁰ and may be compared to the C_{3v} structure computed for CH≡MoH₃,⁸ all bond lengths of CH≡NbH₂F⁻ are longer than those predicted for the isoelectronic neutral CH≡MoH₂F molecule, most particularly the C≡Mo bond (1.719 Å).

Agostic interaction between one of the α-hydrogen atoms and the transition-metal atom is evident in the structure of CH₂=NbHF in the doublet ground state. The CH₂ group is markedly distorted (∠H₁-C-Nb = 92.4° and C-H bond lengths 1.118, 1.081 Å), while the molecule is planar. The agostic angle (92.4°) is compared with 84.5° and 95.1° values for CH₂=MoHF¹⁰ and CH₂=ZrHF² calculated at the same level of theory, indicating that the agostic interaction of the methyldene fluoride complex increases with atomic number among the early second row transition-metals. The natural electron configurations of the valence shell of the carbon atom in CH₂=ZrHF, CH₂=NbHF, and CH₂=MoHF are 2s^{1.32}2p^{3.74}, 2s^{1.28}2p^{3.55}, and 2s^{1.24}2p^{3.38}, respectively, and those of the transition-metal atoms are 5s^{0.26}4d^{1.92}, 5s^{0.48}4d^{3.11}, and 5s^{0.62}4d^{4.65}, respectively. The C=M bond length also decreases in this series (1.966, 1.891, 1.838 Å), respectively. Mulliken charges are given in Table 6. Notice the major change is more positive charge on M and more negative charge on F in CH₂=MoHF for the stronger agostic interaction. Thus, the presence of fluorine has reversed the trend for CH₂=ZrH₂ (92.9° angle, + 1.59 on Zr) and CH₂=MoH₂ (113.0° angle, + 1.26 on Mo).^{2,10}

The agostic interaction is traditionally depicted as coordination of nearby hydrogen atom to the electron-deficient transition

Table 6. Mulliken Charges and Structural Parameters Calculated for the CH₂=MHF Methylenes (M = Zr, Nb, and Mo)^a

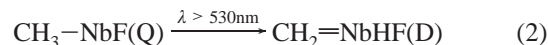
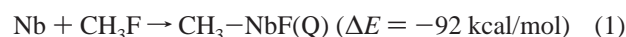
	CH ₂ =ZrHF	CH ₂ =NbHF	CH ₂ =MoHF
q(C)	-0.84	-0.78	-0.74
q(H ₁)	0.16	0.02	0.03
q(H ₂)	0.14	0.00	0.01
q(M)	1.33	1.80	1.68
q(H ₃)	-0.20	-0.43	-0.33
q(F)	-0.59	-0.61	-0.66
C=M (Å)	1.966	1.891	1.838
angle H ₁ -C-M (deg)	95.1	92.4	86.3

^a B3LYP/6-311++G(3df,3pd)/SDD.

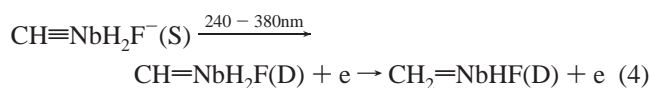
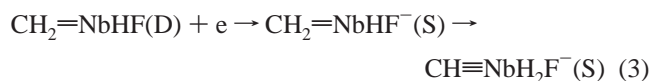
metal atom in a complex.³⁷ In a recent review, Scherer and McGrady reinterpreted the agostic interaction as distortion of chemical bonds and angles in order to stabilize the carbon-metal double bond.³⁸ While agostic interactions have been found to be quite common among d⁰-complexes, the agostic interaction needs to be studied in more detail for small molecules.

Recent work has shown that the agostic interaction decreases with increasing C=M bond length among simple group IV transition-metal (Ti, Zr, and Hf) methylenes CH₂=MHF and CH₂=MH₂.^{1-3,5-7,9} More recently, it has also been reported that the agostic interaction increases in a series of CH₂=TiHX (X = H, F, Cl, and Br), where the computed C=Ti bond length varies from 1.814 to 1.798 and the measured C=Ti stretching frequency increases.⁴ The previous and present results for simple methyldene transition-metal complexes support the notion that the agostic interaction increases with decreasing carbon-metal bond length, where the electron deficiency of the transition-metal plays its own role.

Reactions Occurring in the Matrix. The relative product energies summarized in Figure 4 govern the reaction products observed here. The primary reaction 1 gives the most stable insertion product in the quartet ground state. Rearrangement by α-H transfer to the isoergic methyldene complex is fostered on irradiation with λ > 530 nm light.



Electrons produced in the ablation process²⁴ are apparently captured with high cross section by the doublet methyldene to form the singlet methyldene anion, which rearranges by another α-H transfer to the more stable singlet methyldyne anion, reaction 3. Ultraviolet photodetachment apparently forms the CH=NbH₂F radical intermediate, which undergoes α-H transfer back to the more stable methyldene product, as illustrated by the spectra (Figure 1b-d).



Conclusions

Reactions of laser-ablated Nb atoms with methyl fluoride in excess argon have been carried out during condensation at 8

(36) Jaffart, J.; Etienne, M.; Maseras, F.; McGrady, J. E.; Eisenstein, O. *J. Am. Chem. Soc.* **2001**, *123*, 6000 (C-Nb bond length).

(37) Pillet, S.; Wu, G.; Kulsomphob, V.; Harvey, B. G.; Ernst, R. D.; Coppens, P. *J. Am. Chem. Soc.* **2003**, *125*, 1937.

(38) Scherer, W.; McGrady, G. S. *Angew. Chem., Int. Ed.* **2004**, *43*, 1782.

K. Three groups of product absorptions are observed and assigned to $\text{CH}_3\text{-NbF}$, $\text{CH}_2\text{=NbHF}$, and $\text{CH}\equiv\text{NbH}_2\text{F}^-$ in the lowest $^4\text{A}''$, $^2\text{A}'$, and $^1\text{A}'$ states, respectively, on the basis of the behaviors upon photolysis, annealing, and the addition of CCl_4 as an electron trap. $\text{CH}_3\text{-NbF}$ disappears upon visible irradiation, whereas the monohydrido methylidene complex, $\text{CH}_2\text{=NbHF}$, increases upon both visible and UV irradiations. The dihydrido anionic complex, $\text{CH}\equiv\text{NbH}_2\text{F}^-$, slightly increases upon visible photolysis, but depletes almost completely upon UV irradiation or addition of CCl_4 . The assignments are confirmed by isotopic substitution and excellent agreement of the observed frequencies and isotopic shifts with the calculated values. DFT computation gives a distorted $\text{CH}_2\text{=NbHF}$ structure owing to agostic interaction. The magnitude of agostic interac-

tion appears in increasing order for $\text{CH}_2\text{=ZrHF}$, $\text{CH}_2\text{=NbHF}$, and $\text{CH}_2\text{=MoHF}$ with increasing metal charge and decreasing C=M bond length. Group V transition-metal methylidyne systems are rare, and $\text{CH}\equiv\text{NbH}_2\text{F}^-$ is believed to be the first anionic group V transition-metal methylidyne. The present results show that like group IV and VI transition metals, the group V transition-metal niobium readily forms the C-F insertion product and the resulting methylidene complex in the reaction with methyl fluoride.

Acknowledgment. We gratefully acknowledge financial support from NSF Grant No. CHE 03-52487 to L.A.

OM0507777